

Node classification for signed networks using diffuse interface methods*

Jessica Bosch[†], Pedro Mercado^{‡§}, and Martin Stoll[¶]

Abstract. Signed networks are a crucial tool when modeling *friend and foe* relationships. In contrast to classical undirected, weighted graphs, the edge weights for signed graphs are positive and negative. Crucial network properties are often derived from the study of the associated graph Laplacians. We here study several different signed network Laplacians with a focus on the task of classifying the nodes of the graph. We here extend a recently introduced technique based on a partial differential equation defined on the signed network, namely the *Allen-Cahn-equation*, to classify the nodes into two or more classes. We illustrate the performance of this approach on several real-world networks.

Key words. Signed networks, semi-supervised learning, Phase-field methods, Graph Laplacian

AMS subject classifications. 65F15, 65F10, 65F50, 93C20, 62F15

1. Introduction. The classification of high-dimensional data on graphs is a fundamental problem in many application areas [41, 45, 48]. A technique that has recently been proposed with very promising results utilizes techniques known from partial differential equations in materials science and combines these with graph based quantities (cf. [3]). In particular, the authors use diffuse interface methods that are derived from the Ginzburg–Landau energy. These techniques are well established when one wants to model the phase separation in rapid cooling processes [1, 4, 21, 43]. These methods have been used in image inpainting where a damaged region of an image has to be restored given information about the undamaged image parts. Consequently, the equivalent problem in the context of machine learning, specifically in semi-supervised learning, interprets the undamaged part of an image as labeled data and the damaged region as unlabeled data to be classified. With this analogy, one can readily use results from [2] for the classification problem on graphs. While the materials science problems are typically posed in an infinite-dimensional setup, the corresponding problem in the data classification problem uses the graph Laplacian. This technique has shown great potential and has recently been extended to different setups [6, 19, 37].

In this work, we show that the method by Bertozzi and Flenner [3] can be extended to signed networks. Signed networks are often found in social media and have attracted much attention recently [15, 29, 30, 31, 32, 36, 42] due to its capability to encode different kinds of interactions between observations, even though they have been considered much earlier (cf. [22] for example). The difference to the classical setup where only non-negative edges are used and

*Submitted to the editors DATE.

Funding: This work was funded by the Fog Research Institute under contract no. FRI-454.

[†]Department of Computer Science, The University of British Columbia, 201-2366 Main Mall, Vancouver, BC V6T 1Z4, Canada, (jessica.bosch@ubc.ca)

[‡]Department of Mathematics and Computer Science, Saarland Informatics Campus, Saarland University, Germany, (pedro@cs.uni-saarland.de)

[§]Department of Computer Science, University of Tübingen, Germany

[¶]Technische Universität Chemnitz, Faculty of Mathematics, Professorship Scientific Computing, 09107 Chemnitz, Germany, (martin.stoll@mathematik.tu-chemnitz.de)

thus only encode positive relationships like similarity and friendship, is the use of negative edge weights which encode dissimilarity, conflicts, or enmity relationships, and hence the definition of standard quantities like the graph Laplacian are less straightforward. Several extensions of the graph Laplacian to signed networks have been proposed [10, 30, 36]. In this paper we study how the information of positive and negative edges can be used through different signed Laplacians within the Ginzburg–Landau framework of Bertozzi and co-authors.

The paper is structured as follows. We first introduce the tools needed from graphs and how they are extended to signed networks. We study the properties of the several different signed Laplacians. We then introduce a diffuse interface technique in their classical setup and illustrate how the signed Laplacians can be used within the diffuse interface approach. This is then followed by several extensions in the graph-based Ginzburg–Landau energy. Namely, vector-valued phase fields corresponding to the multi-class segmentation problem as well as the use of non-smooth potentials that can even further improve the clustering behavior. The performance is then illustrated on several examples.

2. Graph information and signed networks. The underlying information for signed and standard networks in general will be represented in the graph Laplacian. We now introduce the Laplacian for a standard network followed by particular versions used for signed networks.

2.1. The combinatorial Graph Laplacian for standard graphs. We consider an undirected graph $G = (V, E)$ consisting of a vertex or node set $V = \{x_i\}_{i=1}^n$ and the edge set E (cf. [11]). Every edge $e \in E$ consists of a pair of nodes (x_i, x_j) with $x_i \neq x_j$ and $x_i, x_j \in V$. If the graph is weighted then we define a weigh function $w : V \times V \rightarrow \mathbb{R}$ with $w(x_i, x_j) = w(x_j, x_i)$ for all i, j in an undirected graph. This function is positive for existing edges and zero otherwise. The degree of the vertex $x_i \in V$ is defined as

$$d(x_i) = \sum_{x_j \in V} w(x_i, x_j).$$

The diagonal degree matrix $D \in \mathbb{R}^{n,n}$ is defined as $D_{i,i} = d(x_i)$. One can then define the graph Laplacian L which is defined via

$$L(x_i, x_j) = \begin{cases} d(x_i) & \text{if } x_i = x_j, \\ -w(x_i, x_j) & \text{otherwise.} \end{cases}$$

We can write $L = D - W$ with the entries of the weight matrix $w_{i,j}$ given by $w(x_i, x_j)$. We typically use normalized versions of the Laplacian [45] such as

$$L_s = D^{-1/2} L D^{-1/2} = I - D^{-1/2} W D^{-1/2},$$

which is a symmetric matrix. The Laplacian matrices L and L_s are positive semidefinite, and the multiplicity of the eigenvalue zero is equal to the number of connected components in the graph [45].

Additionally, one can also use the so-called signless Laplacian defined by

$$Q = D + W$$

and its normalized version

$$Q_s = D^{-1/2} Q D^{-1/2} = I + D^{-1/2} W D^{-1/2}.$$

The signless Laplacians Q and Q_s are positive semi-definite, and the smallest eigenvalue is equal to zero if and only if the graph has a bipartite component [12].

2.2. Graph Laplacians for signed networks. As in the case for a standard graph, we consider a signed graph or network that is undirected. Such graphs have received much attention recently and we refer to [25, 30, 32] among others. Also here, this network consists of n nodes collected in $V = \{x_i\}_{i=1}^n$ but the weights of the edges $e \in E$ that are collected in the adjacency matrix W are allowed to be negative. In more detail, it holds that

$$w_{i,j} = \begin{cases} 1 & \text{if } i \text{ and } j \text{ have a positive relationship,} \\ -1 & \text{if } i \text{ and } j \text{ have a negative relationship,} \\ 0 & \text{if } i \text{ and } j \text{ have an unknown relationship.} \end{cases}$$

Some of the challenges of defining a graph Laplacian based on this weight matrix are summarized in [26]. For example, the definition of the Fiedler vector becomes unclear, possible zero diagonal entries in the degree matrix D , and important for our application the interpretation of $u^T L u$ as an energy.

It has hence been proposed in [30] to replace the traditional graph Laplacian by a signed Laplacian

$$L_{SR} = \bar{D} - W$$

where W is the adjacency or weight matrix and the diagonal degree matrix \bar{D} is defined as

$$\bar{D}_{i,i} = \sum_{j=1}^n |w_{i,j}|.$$

There exist several versions of the Laplacian and we here mention the normalized signed Laplacian

$$L_{SN} = I - \bar{D}^{-1/2} W \bar{D}^{-1/2}.$$

The matrix L_{SR} is also called the *signed-ratio Laplacian* and L_{SN} the *signed-ratio normalized Laplacian*. Further extensions of the graph Laplacians to signed networks have been proposed, for instance the Balance Normalized Laplacian [10] and the geometric mean of Laplacians [36]. We want to study the energy based on L_{SR} and L_{SN} . In more detail, one can define the energy (cf. [30, 18])

$$(2.1) \quad u^T L_{SR} u = \frac{1}{2} \sum_{i,j=1}^n |w_{i,j}| (u_i - \text{sgn}(w_{i,j}) u_j)^2.$$

The last expression also clearly indicates that the signed Laplacian is symmetric and positive semidefinite. We now want to consider the partitioning of V into two disjoint index sets A

and \hat{A} , i.e. the goal of the classification algorithm. The vector u is hence 1 for all indices in A and -1 in \hat{A} . We then evaluate the energy (2.1) and use (2.2)

$$\text{links}^+(A, B) = \sum_{\substack{i \in A, j \in B \\ w_{i,j} > 0}} w_{i,j}, \quad \text{links}^-(A, B) = \sum_{\substack{i \in A, j \in B \\ w_{i,j} < 0}} -w_{i,j}, \quad \text{cut}(A, B) = \sum_{\substack{i \in A, j \in B \\ w_{i,j} \neq 0}} |w_{i,j}|.$$

We consider the following cases for the right hand side of (2.1):

- Here $u_i = u_j = 1$ and hence

$$E_1 = \frac{1}{2} \sum_{i,j \in A} |w_{i,j}| (1 - \text{sgn}(w_{i,j}))^2 = \sum_{\substack{i,j \in A \\ w_{i,j} < 0}} -2w_{i,j} = 2 \text{links}^-(A, A).$$

- Here $u_i = 1$ and $u_j = -1$ and hence

$$E_2 = \frac{1}{2} \sum_{i \in A, j \in \hat{A}} |w_{i,j}| (1 + \text{sgn}(w_{i,j}))^2 = \sum_{\substack{i \in A, j \in \hat{A} \\ w_{i,j} > 0}} 2w_{i,j} = 2 \text{links}^+(A, \hat{A}).$$

- Here $u_i = -1$ and $u_j = 1$ and hence

$$E_3 = \frac{1}{2} \sum_{i \in \hat{A}, j \in A} |w_{i,j}| (-1 - \text{sgn}(w_{i,j}))^2 = \sum_{\substack{i \in \hat{A}, j \in A \\ w_{i,j} > 0}} 2w_{i,j} = 2 \text{links}^+(\hat{A}, A).$$

- Here $u_i = -1$ and $u_j = -1$ and hence

$$E_4 = \frac{1}{2} \sum_{i,j \in \hat{A}} |w_{i,j}| (-1 + \text{sgn}(w_{i,j}))^2 = \sum_{\substack{i \in \hat{A}, j \in \hat{A} \\ w_{i,j} < 0}} -2w_{i,j} = 2 \text{links}^-(\hat{A}, \hat{A}).$$

Noting that $E_2 = E_3$ and putting everything together we have obtained that

$$(2.3) \quad u^T L_{SR} u = E_1 + E_2 + E_3 + E_4 = 2(2 \text{links}^+(A, \hat{A}) + \text{links}^-(A, A) + \text{links}^-(\hat{A}, \hat{A})).$$

From this we see that the quantity $u^T L_{SR} u$ is minimal if the number positive edges between A and \hat{A} (i.e., $\text{links}^+(A, \hat{A})$) and the number of negative edges inside A and \hat{A} (i.e., $\text{links}^-(A, A)$ and $\text{links}^-(\hat{A}, \hat{A})$, respectively) are minimized. This means that as few conflicts as possible should be assigned to the same cluster. In accordance with [18] and more in line with the vector-valued formulation of the Ginzburg–Landau energy in Section 3.2, we define the vector u as being 1 in A and 0 in \hat{A} . Using this, the above four energies are then given as follows:

- Here $u_i = u_j = 1$ and hence

$$E_1 = \frac{1}{2} \sum_{i,j \in A} |w_{i,j}| (1 - \text{sgn}(w_{i,j}))^2 = \sum_{\substack{i,j \in A \\ w_{i,j} < 0}} -2w_{i,j} = 2 \text{links}^-(A, A).$$

- Here $u_i = 1$ and $u_j = 0$ and hence

$$E_2 = \frac{1}{2} \sum_{i \in A, j \in \hat{A}} |w_{i,j}| (1)^2 = \frac{1}{2} \sum_{i \in A, j \in \hat{A}} |w_{i,j}| = \frac{1}{2} \text{cut}(A, \hat{A}).$$

- Here $u_i = 0$ and $u_j = 1$ and hence

$$E_3 = \frac{1}{2} \sum_{i \in \hat{A}, j \in A} |w_{i,j}| (-\text{sgn}(w_{i,j}))^2 = \frac{1}{2} \sum_{i \in \hat{A}, j \in A} |w_{i,j}| = \frac{1}{2} \text{cut}(\hat{A}, A).$$

- Here $u_i = u_j = 0$ and hence

$$E_4 = \frac{1}{2} \sum_{i,j \in \hat{A}} |w_{i,j}| (0)^2 = 0,$$

and thus $u^T L_{SR} u = E_1 + E_2 + E_3 + E_4 = \text{cut}(\hat{A}, A) + 2 \text{links}^-(A, A)$. These non-negative vectors are in fact used when we discuss classification with multiple classes. In contrast to the above approach the authors in [10, 18, 30] consider a normalized cut criteria for signed networks that is used for separating the nodes into clusters of roughly the same size and it follows from the minimization of the generalized Rayleigh quotient

$$\frac{u^T L_{SR} u}{u^T \bar{D} u},$$

which is equivalent to minimizing

$$\frac{\tilde{u}^T \bar{D}^{-1/2} L_{SR} \bar{D}^{-1/2} \tilde{u}}{\tilde{u}^T \tilde{u}} = \frac{\tilde{u}^T L_{SN} \tilde{u}}{\tilde{u}^T \tilde{u}},$$

with $\tilde{u} = \bar{D}^{1/2} u$. The energy for the normalized Laplacian is then given by

$$(2.4) \quad u^T L_{SN} u = \frac{1}{2} \sum_{i,j=1}^n |w_{i,j}| \left(\frac{u_i}{\bar{D}_{i,i}} - \text{sgn}(w_{i,j}) \frac{u_j}{\bar{D}_{j,j}} \right)^2.$$

For more details we refer to [18]. As observed in [36] we note that using the matrices above for the graph with positive edges and the one with negative edges we can write

$$L_{SR} = L^+ + Q^-$$

with L^+ the Laplacian for the graph consisting of the positive edges and Q^- the signless Laplacian for the graph of negative edges. Another useful Laplacian is obtained as the arithmetic mean of the normalized matrices L_s^+ and Q_s^- to obtain

$$L_{AM} = L_s^+ + Q_s^-.$$

3. Diffuse interface methods. In the field of materials science, diffuse interface methods have been used with great success [1, 4, 8, 16, 20]. Beyond the use to simulate phase separation, these techniques can be found in many other areas from biomembrane simulation [46] to image inpainting [2, 5].

Recently, Bertozzi and Flenner [3] have shown how these methods can be extended to semi-supervised learning based on underlying graphs. The derivation of classical models such as the Allen–Cahn [1] or Cahn–Hilliard equations [8] is typically obtained from a gradient flow of the Ginzburg–Landau energy

$$(3.1) \quad E(u) = \int \frac{\varepsilon}{2} |\nabla u|^2 dx + \int \frac{1}{\varepsilon} \psi(u) dx$$

where u is the phase-field and ε the interface parameter, which is typically assumed to be small. The function $\psi(u)$ is a potential that forces the phase-field u to take values at either $u \approx -1$ or $u \approx 1$. In the learning framework this corresponds to a separation into two clusters, see the discussion above. The minimization of the energy $E(u)$ follows a gradient flow, which leads to the well-known Allen–Cahn equation written as

$$(3.2) \quad \partial_t u = \varepsilon \Delta u - \varepsilon^{-1} \psi'(u)$$

with a given initial condition u_0 and zero Neumann boundary conditions. Here, $\psi'(u)$ is the derivative of a smooth potential $\psi(u)$. The Allen–Cahn equation has also been used very successfully in image inpainting [13, 34]. For this purpose, Equation (3.2) is modified

$$(3.3) \quad \partial_t u = \varepsilon \Delta u - \varepsilon^{-1} \psi'(u) + \omega(x)(f - u)$$

where $\omega(x)$ is a parameter that is zero in the damaged image domain D and typically a large constant ω_0 in the intact parts $\Omega \setminus D$. Here f is the given image that we do not want to change in the undamaged part. This is also the crucial idea by Bertozzi and Flenner [3]. The undamaged part of the image in the semi-supervised learning context corresponds to the given information that we have learned and want to use as a basis to classify the remaining instances.

In practice, often more than two components occur and this is the goal for multi-class classification. For this purpose, the Ginzburg–Landau energy for two components in (3.1) generalizes to

$$(3.4) \quad E(u) = \int \frac{\varepsilon}{2} \sum_{i=1}^K |\nabla u_i|^2 dx + \int \frac{1}{\varepsilon} \psi(u) dx$$

for $K > 2$ components. Here, $u = (u_1, \dots, u_K)^T$ is now the vector-valued phase-field, and the potential function $\psi(u)$ has K distinct minima instead of two. The smooth potential in the scalar case generalizes to the vector-valued case as $\psi(u) = \frac{1}{4} \sum_{i=1}^K u_i^2 (1 - u_i)^2$. We also use this approach to cluster the given data into K classes. This follows from the modified Allen–Cahn equation given above in its vector-valued form (cf. [7] for the use within image inpainting). We are now introducing the corresponding problem utilizing the graph information and in particular that of a signed network.

3.1. Diffuse interface methods on graphs. Bertozzi and Flenner [3] formulated the semi-supervised learning problem based on the inpainting formulation (3.3). We now define (3.3) using the signed network information via the underlying graph Laplacian L_{SN} to give

$$(3.5) \quad E(u) = \frac{\varepsilon}{2} u^T L_{SN} u + \sum_{x \in V} \frac{1}{4\varepsilon} (u(x)^2 - 1)^2 + \sum_{x \in V} \frac{\omega(x)}{2} (f(x) - u(x))^2.$$

We solve such an equation employing a convexity splitting scheme (see [2, 5, 6, 17, 35, 40, 44])

$$E(u) = E_1(u) - E_2(u)$$

with

$$E_1(u) = \frac{\varepsilon}{2} u^T L_{SN} u + \frac{c}{2} u^T u$$

and

$$E_2(u) = \frac{c}{2} u^T u - \sum_{x \in V} \frac{1}{4\varepsilon} (u(x)^2 - 1)^2 - \sum_{x \in V} \frac{\omega(x)}{2} (f(x) - u(x))^2.$$

In order to guarantee the convexity of the energy terms, we require $c \geq \omega_0 + \frac{1}{\varepsilon}$; see, e.g., [6]. One proceeds with the use of an implicit Euler scheme for E_1 and explicit treatment for E_2 . We did not introduce an index for the temporal discretization but assume all values $u(x)$ are evaluated at the new time-point whereas \bar{u} gives information from the previous time. These equations are a model based on the infinite-dimensional formulation but our goal is to use the signed-network graph Laplacian based formulation as introduced in [3]. In the graph based framework we get

$$\frac{u - \bar{u}}{\tau} + \varepsilon L_{SN} u + cu = cu - \sum_{x \in V} \frac{1}{\varepsilon} u(x)(u(x)^2 - 1) + \sum_{x \in V} \omega(x)(f(x) - u(x)).$$

For (λ_l, ϕ_l) , $l = 1, \dots, k$, being the k smallest eigenpairs of L_{SN} , we obtain

$$(3.6) \quad \frac{u_l - \bar{u}_l}{\tau} + \varepsilon \lambda_l u_l + cu_l = -\frac{1}{\varepsilon} \bar{b}_l + c \bar{u}_l + \bar{d}_l$$

where $\bar{b} = \psi' \left(\sum_{l=1}^k \bar{u}_l \phi_l \right)$ and $\bar{d} = \omega \left(f - \sum_{l=1}^k \bar{u}_l \phi_l \right)$. Equivalently, we can write this as

$$(3.7) \quad (1 + \varepsilon \tau \lambda_l + c \tau) u_l = \frac{\tau}{\varepsilon} \bar{b}_l + (1 + c \tau) \bar{u}_l + \tau \bar{d}_l \quad \forall l.$$

With this scheme we can implement the graph-based Allen-Cahn equation for signed networks. Ginzburg-Landau based graph segmentation has recently seen many exciting developments [19, 35, 37, 38, 44]. One of the key questions is the classification into more than two classes, which we discuss next.

3.2. Vector-valued formulation. Garcia-Cardona et al. [19] as well as Merkurjev et al. [37] have extended the use of the diffuse interface model based on the generalized Ginzburg–Landau energy (3.4) to multi-class segmentation of high-dimensional data on graphs. For hypergraphs this was done in [6]. We introduce the matrix $U = (u_1, \dots, u_n)^T \in \mathbb{R}^{n,K}$, where the m th component of the vector $u_i \in \mathbb{R}^K$ indicates the strength for data point i to belong to class m . For each node i , the vector u_i has to be an element of the Gibbs simplex Σ^K

$$\Sigma^K := \left\{ (x_1, \dots, x_K)^T \in [0, 1]^K \left| \sum_{l=1}^K x_l = 1 \right. \right\}.$$

The Ginzburg–Landau energy functional on graphs in (3.5) generalizes to the multi-class case as

$$(3.8) \quad E(U) = \frac{\varepsilon}{2} \text{trace}(U^T L_{SN} U) + \frac{1}{2\varepsilon} \sum_{i \in V} \left(\prod_{l=1}^K \frac{1}{4} \|u_i - \mathbf{e}_l\|_{L_1}^2 \right) + \sum_{i \in V} \frac{\omega}{2} \|\hat{u}_i - u_i\|_{L_2}^2$$

with $\hat{U} = (\hat{u}_1, \dots, \hat{u}_n)^T$ representing the learned data and $\mathbf{e}_l \in \mathbb{R}^K$ being the vector whose l th component equals one and all other components vanish. Note that the vectors $\mathbf{e}_1, \dots, \mathbf{e}_K$ correspond to the pure phases. The authors in [19, 37] use an L_1 -norm for the potential term (the middle term in (3.8)) since it prevents an undesirable minimum from occurring at the center of the simplex, as it would be the case with an L_2 -norm for large K . The same convexity splitting scheme as in Section 3.1 is used to minimize the Ginzburg–Landau functional in the phase-field approach. This results in

$$(3.9) \quad \frac{U - \bar{U}}{\tau} + \varepsilon L_{SN} U + cU = -\frac{1}{2\varepsilon} T(\bar{U}) + c\bar{U} + \omega(\hat{U} - \bar{U}),$$

where the elements T_{ik} of the matrix $T(\bar{U})$ are given as

$$T_{ik} = \sum_{l=1}^K \frac{1}{2} (1 - 2\delta_{kl}) \|\bar{u}_i - \mathbf{e}_l\|_{L_1} \prod_{m=1, m \neq l}^K \frac{1}{4} \|\bar{u}_i - \mathbf{e}_m\|_{L_1}^2.$$

The parameter $c \geq \omega_0 + \frac{1}{\varepsilon}$ arises from the convexity splitting. As before, we assume that U is evaluated at the new time-point, whereas \bar{U} indicates the previous time-point. Using the eigendecomposition $L_{SN} = \Phi \Lambda \Phi^T$ and multiplying (3.9) by Φ^T from the left, we obtain

$$(3.10) \quad \mathcal{U} = B^{-1} \left[(1 + c\tau) \bar{\mathcal{U}} - \frac{\tau}{2\varepsilon} \Phi^T T(\bar{U}) + \tau\omega(\hat{\mathcal{U}} - \bar{\mathcal{U}}) \right],$$

where the calligraphic fonts have the meaning $\mathcal{U} = \Phi^T U$ and $\hat{\mathcal{U}} = \Phi^T \hat{U}$. Since $B = (1 + c\tau)I + \varepsilon\tau\Lambda$ is a diagonal matrix with positive entries, its inverse is easy to apply. After the update, we have to project the solution back to the Gibbs simplex Σ^K . In order to do this, we make use of the projection procedure in [9].

For the initialization of the segmentation problem, we first assign random values from the standard uniform distribution on $(0, 1)$ to the nodes. Then, we project the result to the Gibbs simplex Σ^K and set the values in the fidelity points to the pure phases.

Here, we finish the presentation of the model proposed in [19, 37]. Next, we extend the diffuse interface approach to the use of non-smooth potentials using the example of the scalar model. The vector-valued case follows analogously.

3.3. Non-smooth potentials. The potential ψ plays a crucial role for standard phase field problems. Recently [6], these potentials have been shown to also be effective for diffuse interface methods on graphs and hypergraphs. We here propose the use of the well-known obstacle potential. In more detail, we consider

$$(3.11) \quad \psi_{ns}(u) := \begin{cases} \frac{1}{2}(1 - u^2) & -1 \leq u \leq 1, \\ \infty & \text{otherwise,} \end{cases}$$

where $\psi_0(u) := \frac{1}{2}(1 - u^2)$. We now follow a well-known approach by regularizing the energy with the Moreau–Yosida penalty term [7, 23] and obtain

$$E(u_\nu) = \int_{\Omega} \frac{\varepsilon}{2} |\nabla u_\nu|^2 + \frac{1}{\varepsilon} \psi_0(u_\nu) + \frac{1}{2\nu} |\max(0, u_\nu - 1)|^2 + \frac{1}{2\nu} |\min(0, u_\nu + 1)|^2 dx,$$

with ν the penalty parameter. The same convexity splitting scheme as in Section 3.1 is used to minimize the Ginzburg–Landau functional in the phase-field approach, whereas the energy functional E_1 contains in addition the Moreau–Yosida penalty term and the potential function in E_2 becomes $\psi_0(u)$. In order to guarantee the convexity of the two energy terms, we require $c \geq \omega_0$; see, e.g., [6]. This leads to the following evolution equation for the classical problem

$$(3.12) \quad \frac{u_\nu - \bar{u}_\nu}{\tau} - \varepsilon \Delta u_\nu + c u_\nu + \frac{1}{\nu} \max(0, u_\nu - 1) + \frac{1}{\nu} \min(0, u_\nu + 1) = -\frac{1}{\varepsilon} \psi'_0(\bar{u}) + c \bar{u} + \omega(f - \bar{u}).$$

In the non-smooth setting, we obtain a nonlinear relation due to the non-smooth relation given by the maximum and minimum operator, which we treat with the well-known semi-smooth Newton method [24]. For (3.12) written as $F(u_\nu) = 0$, the Newton system is given via

$$u_\nu^{(m+1)} = u_\nu^{(m)} - G(u_\nu^{(m)})^{-1} F(u_\nu^{(m)}), \quad m = 0, 1, \dots$$

We define the sets

$$\begin{aligned} \mathcal{A}(u_\nu) &:= \{x \in \Omega : u_\nu > 1 \text{ or } -u_\nu > 1\}, \\ \mathcal{A}_\pm(u_\nu) &:= \{x \in \Omega : \pm u_\nu > 1\}, \end{aligned}$$

which leads to the Newton system

$$G(u_\nu^{(m)}) u_\nu^{(m+1)} = -\nu^{-1} \left(\chi_{\mathcal{A}_-(u_\nu^{(m)})} - \chi_{\mathcal{A}_+(u_\nu^{(m)})} \right) \mathbf{1} + \left(\frac{1}{\varepsilon} + c + \frac{1}{\tau} \right) \bar{u} + \omega(f - \bar{u})$$

where $G(u_\nu^{(m)}) := (c + \frac{1}{\tau})I - \varepsilon \Delta + \frac{1}{\nu} \chi_{\mathcal{A}(u_\nu^{(m)})}$ with I the identity operator and $\mathbf{1}$ the vector of all ones. The equivalent formulation for signed networks is given via $G(u_\nu^{(m)}) := (c + \frac{1}{\tau})I + \varepsilon L_{SN} + \frac{1}{\nu} \chi_{\mathcal{A}(u_\nu^{(m)})}$. Dropping the index ν and assuming the ansatz $u^{(m)} = \sum_{l=1}^k u_{l,m} \phi_k = \Phi u_{(m)}$, we obtain

$$(3.13) \quad \Phi^T G(u^{(m)}) \Phi u_{(m+1)} = -\frac{1}{\nu} \Phi^T \left(\chi_{\mathcal{A}_-(u^{(m)})} - \chi_{\mathcal{A}_+(u^{(m)})} \right) \mathbf{1} + \left(\frac{1}{\varepsilon} + c + \frac{1}{\tau} \right) \Phi^T \Phi \bar{u} + \Phi^T \omega(f - \Phi \bar{u}),$$

and the main system is defined by the operator

$$\Phi^T G(u^{(m)}) \Phi = \left(c + \frac{1}{\tau} \right) I + \varepsilon \Lambda + \frac{1}{\nu} \Phi^T \chi_{\mathcal{A}(u^{(m)})} \Phi$$

where Λ is the diagonal matrix containing the k eigenvalues used in the approximation. This system is of course rather easily solved in every step of the Newton step but still the non-smooth scheme comes at additional cost in comparison to the smooth potential. Namely, due to the nonlinear iteration performed at every time-step.

4. Numerical experiments. We now illustrate the performance of our scheme for various examples. Before discussing the individual application we want to make some comments on the general setup of our implementation.

The computation of the eigenvalues is based on `eigs` from MATLAB, which is based on the Lanczos process. The methods proposed here contain several parameters that influence the performance of the schemes and we illustrate the performance of the method with respect to varying them. Such parameters include the interface parameter ε , the number of eigenvalues for the Laplacian, the convexity splitting parameter c , the (pseudo) time-step of the Allen–Cahn equation τ , as well as the correct stopping tolerance. One of the crucial questions is also the performance of the algorithms with respect to changes in the number of known or learned data.

Regarding the computational costs for solving the smooth versus the non-smooth model, it is clear that the first one outperforms the latter. In the smooth case, we need to apply the inverse of one diagonal small matrix per time step. In the non-smooth case, we have two additional loops within each time step: These are first a loop over the regularization parameter ν . More precisely, we solve for a sequence $\{\nu_p\}_{p \in \mathbb{N}}$ with $\nu_p \rightarrow 0$. Inside the regularization loop is the semi-smooth Newton iteration, which runs over the Newton step l . Hence, in the non-smooth case, we need to apply the inverse of at most $q_{\max} \cdot l_{\max}$ non-diagonal $k \times k$ matrices per time step, where q_{\max} denotes the length of the regularization parameter sequence and l_{\max} the maximum number of Newton steps.

As a competing approach we compare with the method of [42], which is one of the only methods available that is tailored for signed networks and is called NCSSN in the remainder of this paper. In all experiments, the parameter setting of our method is always the same, unless otherwise stated: the fidelity parameter $\omega_0 = 10^3$, the interface parameter $\varepsilon = 10^{-1}$, the convexity parameter $c = \frac{3}{\varepsilon} + \omega_0$, time step-size $dt = 0.1$, maximum number of iterations is set to 2000, stopping tolerance is 10^{-6} .

4.1. Experiments in Sociology Networks. We evaluate our method based on Laplacians L_{sym}^+ , Q_{sym}^- , L_{SN} , and L_{AM} and compare to NCSSN. The comparison is done through three real-world signed networks: Highland tribes (Gahuku-Gama) network [39], Slovene Parliamentary Parties Network [27] and US Supreme Court Justices Network [14]. For each of these datasets we take as labels the ground truth clustering given in the corresponding references. The parameters of NCSSN here used are: $\lambda = 1, \alpha = 1, \beta = 0.6, \gamma = 0.1$, which are chosen so that overall the best average classification performance is observed in a grid where $\lambda \in \{0, 0.01, 0.1, 0.3, 0.5, 0.7, 1, 10, 100\}$, $\beta \in \{0, 0.1, \dots, 1\}$ and $\gamma \in \{0.1, \dots, 1\}$, together with maximum 100 iterations and stopping tolerance of 10^{-5} .

		Gahuku-Gama		Slovene Parliament		US Supreme Court	
		Avg. Acc	Best(%)	Avg. Acc	Best(%)	Avg. Acc	Best(%)
L_{sym}^+		1.0	100	1.0	100	1.0	100
NCSSN		0.8659	35.71	1.0	100	0.8214	50
ours	Q_{sym}^-	0.5665	0	0.9850	96	0.8571	70
	L_{SN}	0.9967	96.43	1.0	100	1.0	100
	L_{AM}	0.9813	75.71	1.0	100	0.9929	95

Table 1: Average classification accuracy and percentage of cases where the best classification accuracy is obtained with different sets of labeled nodes. Our method based on Laplacians L_{SN} and L_{AM} consistently presents the best classification performance among methods for signed graphs.

We generate all possible sets of labeled nodes, such that from each class only one labeled node is taken. We report the corresponding average classification accuracy, and the percentage of cases where each method returns the largest classification accuracy.

We first observe that in all cases positive relationships in G^+ are informative, as our method based on the Laplacian L_{sym}^+ always returns the highest classification accuracy. For negative relationships in G^- , we can see that this is slightly different, as the classification accuracy based on the signless Laplacian Q_{sym}^- is consistently lower. For the methods based on both positive and negative relationships, we can see that our method using the signed Laplacian L_{SN} shows the best average classification accuracy, followed by our method using the arithmetic mean Laplacian L_{AM} .

As positive relationships are more informative than negative relationships in these datasets, these experiments show how effectively each method blends the information coming from both kinds of relationships.

4.2. Experiments in Wikipedia Datasets. We present experiments on three different real world networks: wikipedia-Elec, wikipedia-RfA, and Wikipedia-Editor. We give a small description of each dataset. Wikipedia-Elec [33] and Wikipedia-RfA [33] are datasets of editors of Wikipedia that request to become administrators, where any Wikipedia member may give a supporting, neutral or opposing vote. From these votes we build a signed network for each dataset, where a positive (resp. negative) edge indicates a supporting (resp. negative) vote by a user and the corresponding candidate. The label of each node in these networks is given by the output of the corresponding request: positive (resp. negative) if the editor is chosen (resp. rejected) to become an administrator. Wikipedia-Editor [47] is extracted from the UMD Wikipedia dataset [28]. The dataset is composed of vandals and benign editors of Wikipedia. There is a positive (resp. negative) edge between users if their co-edits belong the same (resp. different) categories. Each node is labeled as either benign (positive) or vandal (negative).

Experimental setup: the fidelity parameter $\omega_0 = 10^3$, the interface parameter $\varepsilon = 10^{-1}$, the convexity parameter $c = \frac{3}{\varepsilon} + \omega_0$, time step-size $dt = 0.1$, maximum number of iterations is set to 2000, stopping tolerance is 10^{-6} , and the number of runs is 10, i.e. we always show the average classification accuracy of 10 runs. For the following experiments we take the largest

	Wikipedia-RfA			Wikipedia-Elec			Wikipedia-Editor		
	G^+	G^-	G^\pm	G^+	G^-	G^\pm	G^+	G^-	G^\pm
# of nodes	3024	3124	3470	1997	2040	2325	17647	14685	20198
% of + nodes	55.2%	42.8%	48.1%	61.3%	47.1%	52.6%	38.5%	33.5%	36.8%
# of edges	204035	189343	215013	107650	101598	111466	620174	304498	694436
% of + edges	100%	0%	78.2%	100%	0%	77.6%	100%	0%	77.3%

Table 2: Dataset statistics of the largest connected components of G^+ , G^- and G^\pm .

connected component of either G^+ , G^- or G^\pm , depending on the Laplacian used with our method, i.e. for L_{sym}^+ we take the largest connected component of G^+ , for Q_{sym}^- we take the largest connected component of G^- , and for L_{SN} and L_{AM} we take the largest connected component of G^\pm . In Table 2 we show statistics of the corresponding largest connected components of each dataset. We can observe that all datasets present a larger proportion of positive edges than of negative edges in the corresponding signed network G^\pm , i.e. at least 77.3% of edges are positive in all datasets. Further, we can observe that the distribution of positive and negative node labels is balanced, except for Wikipedia-Editor where the class of positive labels is between 33.5% and 38.5% of nodes.

4.2.1. Comparison of Classification Performance. In this set of experiments we first compare our method based on different Laplacians with the state of the art method NCSSN.

Experimental setup: For the state of the arte method NCSSN we set its parameters as follows: maximum number of 100 iterations, stopping tolerance of 10^{-5} and $\lambda = 10^{-2}$. The choice of λ is done by analyzing the performance of NCSSN with different values of λ , namely $\{0, 0.01, 0.1, 0.3, 0.5, 0.7, 1, 10, 100\}$. The best global performance across all datasets is achieved with $\lambda = 10^{-2}$, which is the value that we use in all experiments. Further, we set the number of latent dimensions to be equal to the number of eigenvectors given to our proposed method.

Results: In Table 3 we present the corresponding results for the case where different amounts of labeled nodes are given, while the number of eigenvectors is fixed to 20 for datasets Wikipedia-RfA and Wikipedia-Elec, and to 200 for Wikipedia-Editor. We can observe that our method consistently outperforms other approaches when both positive and negative edges are considered. In particular we can see from L_{sym}^+ and Q_{sym}^- that in many cases negative edges are more informative than positive ones, inducing a large classification accuracy. Further, we can observe that the best performance comes from our method based on L_{SN} and L_{AM} , where both positive and negative are considered, showing that in deed our method is able to take advantage of the signed Laplacian information blending effect. Moreover, we can see that our method based on the signed Laplacian L_{AM} presents a consistent gap with respect to the state of the art method NCSSN. This gaps goes from 4% to 61%.

4.2.2. Effect of the Number of Eigenvectors. We now study how the performance of our method is affected by the number of eigenvectors given through different Laplacians. **Experimental setup:** we fix the amount of labeled nodes to 5% and consider different amounts of given eigenvectors. For datasets Wikipedia-RfA and Wikipedia-Elec we set the number of given eigenvectors N_e in the range $N_e = 1, \dots, 100$ and for Wikipedia-Editor in the

		Wikipedia-RfA				Wikipedia-Elec				Wikipedia-Editor			
		1%	5%	10%	15%	1%	5%	10%	15%	1%	5%	10%	15%
L_{sym}^+		0.58	0.60	0.60	0.60	0.61	0.65	0.64	0.64	0.82	0.84	0.84	0.84
NCSSN		0.76	0.79	0.80	0.81	0.70	0.80	0.80	0.83	0.49	0.55	0.57	0.57
ours	Q_{sym}^-	0.79	0.80	0.80	0.80	0.71	0.76	0.76	0.77	0.74	0.76	0.76	0.77
	L_{SN}	0.68	0.75	0.76	0.76	0.81	0.84	0.85	0.85	0.83	0.84	0.85	0.85
	L_{AM}	0.85	0.85	0.85	0.85	0.88	0.89	0.89	0.89	0.79	0.81	0.81	0.82

Table 3: Average classification accuracy with different amounts of labeled nodes. We fix the number of eigenvectors to 20 for datasets Wikipedia-RfA and Wikipedia-Elec and 200 for Wikipedia-Editor. Average accuracy is computed out of 10 runs. Our method based on Laplacians L_{SN} and L_{AM} consistently presents the best classification performance.

range $N_e = 1, 10, \dots, 1000$. The average classification accuracy is shown in Fig. 1.

Results: for Wikipedia-RfA and Wikipedia-Elec we can see that the classification accuracy of our method based on the Laplacian Q_{sym}^- outperforms our method based on the Laplacian L_{sym}^+ by a meaningful margin, suggesting that for the task of node classification negative edges are more informative than positive edges. Further, we can see that our method based on the arithmetic mean Laplacian L_{AM} consistently shows the highest classification accuracy indicating that taking into account the information coming from both positive and negative edges is beneficial for classification performance.

For the case of Wikipedia-Editor the previous distinctions are not clear anymore. For instance, we can see that the performance of our method based on the Laplacian L_{sym}^+ outperforms the case with Q_{sym}^- . Moreover, the information coming from positive edges presents a more prominent performance, being competitive to our method based on the Laplacian L_{SN} when the number of eigenvectors is relatively small, whereas the case with the arithmetic mean Laplacian L_{AM} presents a larger classification accuracy for larger amounts of eigenvectors.

Finally, we can see that in general our method first present an improvement in classification accuracy, reaches a maximum and then decreases with the amount of given eigenvectors.

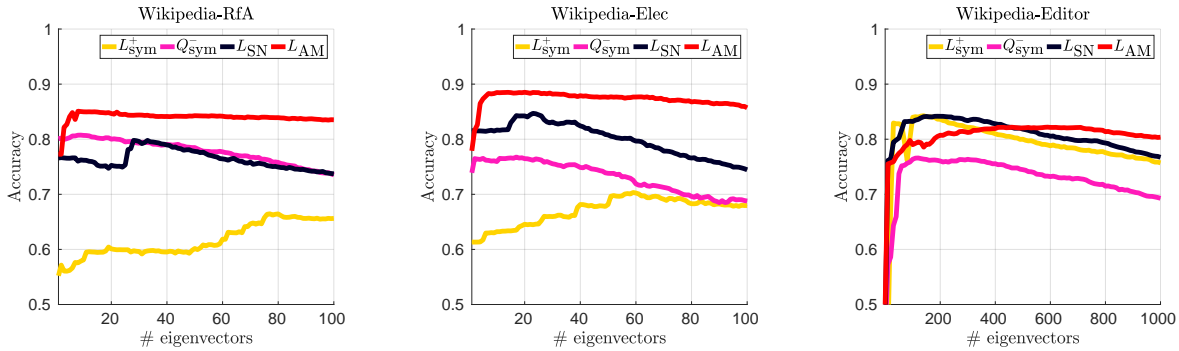


Figure 1: Average classification accuracy with 5% labeled nodes and different amounts of eigenvectors. Average accuracy is computed out of 10 runs. Our method based on Laplacians L_{SN} and L_{AM} consistently presents the best classification performance.

4.2.3. Effect of the Number of Labeled Nodes. We now study how the classification accuracy of our method is affected by the amount of labeled nodes.

Experimental setup: we fix the amount of eigenvectors to $N_e \in \{20, 40, 60, 80, 100\}$ for Wikipedia-RfA and Wikipedia-Elec, and $N_e \in \{200, 400, 600, 800, 1000\}$ for Wikipedia-Editor. Given N_e , we evaluate our method with different proportions of labeled nodes, going from 1% to 25% of the number of nodes $|V|$.

Results: The corresponding average classification accuracy is shown in Fig. 2. As expected, we can observe that the classification accuracy increases with larger amounts of labeled nodes. Further, we can observe that this effect is more pronounced when larger amounts of eigenvectors N_e are taken, i.e. the smallest classification accuracy increment is observed when the number of eigenvectors N_e is 20 for Wikipedia-RfA and Wikipedia-Elec and 100 eigenvectors for Wikipedia-Editor.

Further, we can observe that overall our method based on the signed normalized Laplacian L_{SN} and the arithmetic mean Laplacian L_{AM} performs best, suggesting that blending the information coming from both positive and negative edges is beneficial for the task of node classification.

While our method based on signed Laplacians L_{SN} and L_{AM} overall presents the best performance, we can observe that they present a slightly difference when it comes to its sensibility to the amount of labeled nodes. In particular, we can observe how the increment on classification accuracy of the signed normalized Laplacian L_{SN} is rather clear, whereas with the arithmetic mean Laplacian L_{AM} the increment is smaller. Yet, L_{AM} systematically presents a better classification accuracy when the amount of labeled nodes is limited.

4.2.4. Joint Effect of the Number of Eigenvectors and Amount of Labeled Nodes. We now study the joint effect of the number of eigenvectors and the amount of labeled nodes in the classification performance of our method based on the signed normalized Laplacian L_{SN} .

Experimental setup: We let the the number of eigenvectors $N_e \in \{10, 20, \dots, 100\}$ for datasets Wikipedia-RfA and Wikipedia-Elec and $N_e \in \{100, 200, \dots, 1000\}$ for dataset Wikipedia-Editor. Further, we let the amount of labeled nodes to go from 1% to 25%, we set the fidelity parameter to $\omega_0 = 10^3$ and the interface parameter to $\varepsilon = 10^{-1}$.

Results: The corresponding results are shown in Fig. 3, where we confirm that the classification accuracy consistently increases with larger amounts of labeled nodes. Finally, we can notice that the classification accuracy first increases with the amount of eigenvectors, it reaches a maximum, and then slightly decreases.

To better appreciate the performance of our method under various settings, we present the difference between the lowest and largest average classification accuracy in table 4. We can see that the increments go from 25.13% to 36.54%.

4.2.5. Parameter Analysis. We now study the effect of fidelity (ω_0) and interface (ε) parameters on the classification accuracy of our method based on the signed normalized Laplacian L_{SN} . **Experimental setup:** we fix the number of eigenvectors to $N_e = 20$, and let the amount of labeled nodes to go from 1% to 15%. Further, we set the fidelity parameter ω_0 to take values in $\{10^0, 10^1, \dots, 10^5\}$ and the interface parameter ε to take values in $\{10^{-5}, 10^{-4}, \dots, 10^4, 10^5\}$.

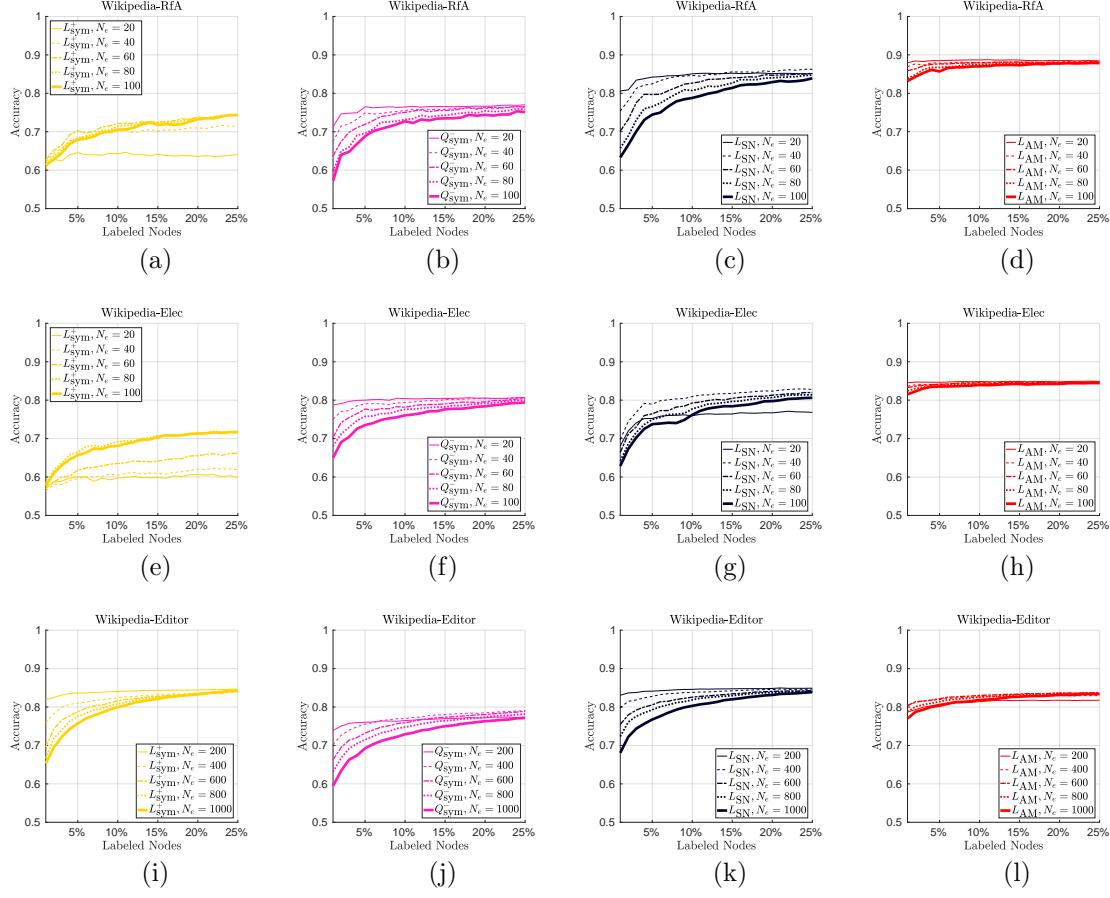


Figure 2: Average classification accuracy with smooth potential with different amount of labeled nodes given a fixed number of eigenvectors. From top to bottom: Each row presents classification accuracy of dataset Wikipedia-RfA, Wikipedia-Elec, and Wikipedia-Editor. From left to right: Each column presents classification accuracy of Laplacians L_{sym}^+ , Q_{sym}^- , L_{SN} , and L_{AM} . Average accuracy is computed out of 10 runs.

Dataset	Lowest Accuracy	Largest Accuracy	Increment
wikipedia-Elec	0.6317	0.8625	36.54%
wikipedia-RfA	0.6264	0.8280	32.17%
wikipedia-Editor	0.6785	0.8491	25.13%

Table 4: Lowest and largest average classification accuracy of L_{SN} per dataset with fidelity parameter $\omega_0 = 10^3$ and interface parameter $\varepsilon = 10^{-1}$. Average accuracy is computed out of 10 runs.

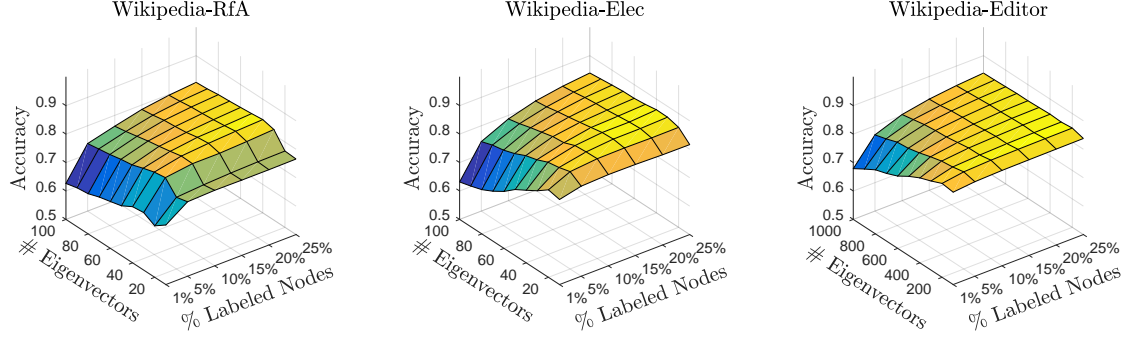


Figure 3: Average classification accuracy of our method with L_{SN} under different number of eigenvectors and different amounts of labeled nodes. Average classification accuracy is taken out of 10 runs.

Results: The corresponding results are shown in Fig. 4. We observe:

First: we can see that the larger the amount of labeled nodes, the smaller is the effect of parameters (ω_0, ε) . In particular, we can observe that when the amount of labels is at least 10% of the number of nodes, then the parameter effect of (ω_0, ε) is small, in the sense that the classification accuracy remains high.

Second: we can see that there is a relationship between the fidelity parameter ω_0 and the interface parameter ε describing a *safe region*, in the sense that the classification accuracy is not strongly affected by the lack of large amounts of labeled nodes. In particular, we can observe that this region corresponds to the cases where the interface parameter ε is larger than the fidelity parameter ω_0 , i.e. $\varepsilon(k_1) > \omega_0(k_2)$ where $\varepsilon(k_1) = 10^{k_1}$ and $\omega_0(k_2) = 10^{k_2}$, with $k_1 \in \{10^0, 10^1, \dots, 10^5\}$ and $k_2 \in \{10^{-5}, 10^{-4}, \dots, 10^4, 10^5\}$. This can be well observed through a slightly triangular region particularly present for the case where the amount of labeled nodes is 1% on all datasets, which is depicted in Figs. 4a, 4e, and 4i.

4.3. Comparing the smooth and non-smooth potential. In this section, we compare the classification effect using the smooth and nonsmooth model applied to the Wikipedia-Elec dataset.

Experimental setup: fidelity parameter $\omega_0 = 10^3$, interface parameter $\varepsilon = 10^{-1}$, convexity parameter $c = \frac{3}{\varepsilon} + \omega_0$, time step-size $\tau = 0.01$, maximum number of iterations of 100, stopping tolerance of 10^{-6} , and $\nu_{\max} = 10^{-7}$.

Results: The corresponding results are shown in Fig. 5. In Figs. 5a and 5b the average classification accuracy is shown of our method based on the non-smooth potential and for Wikipedia-RfA and Wikipedia-Elec, respectively. We can observe that the sensibility towards the different amounts of eigenvectors and labeled nodes is clearly minor in comparison to our method based on the smooth potential (see f.i. Fig. 3). Moreover, there is a clear increase in performance when a small amount of eigenvectors is taken.

Further, a comparison in performance of our method based on smooth and non-smooth potentials is shown in Figs 5c and 5d, where negative values indicate that our non-smooth potential based method out performs its smooth potential counter part. We can see that

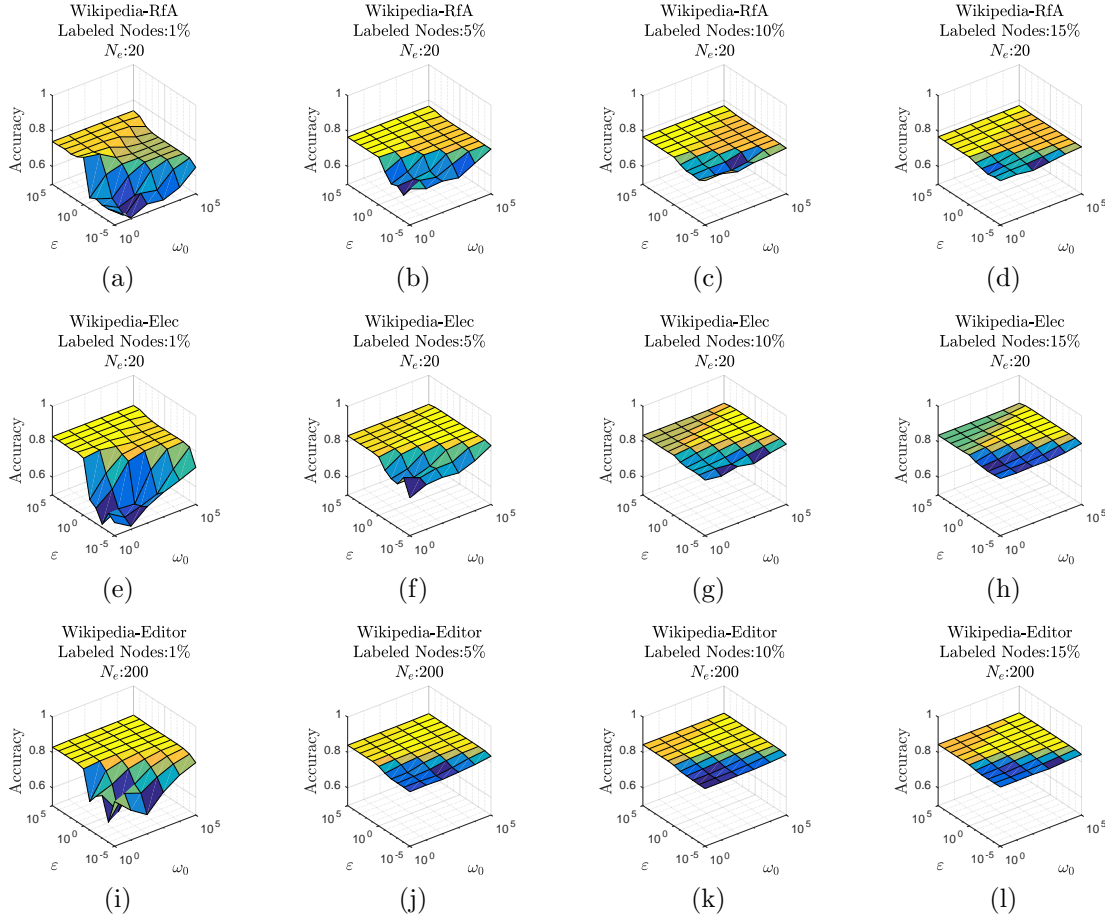


Figure 4: Average classification accuracy of our method based on the signed normalized Laplacian L_{SN} with different values of fidelity (ω_0) and interface (ϵ). Columns (from left to right): amount of labeled nodes: 1%, 5%, 10%, 15%. Rows (from top to bottom): classification accuracy on datasets Wikipedia-RfA, Wikipedia-Elec, and Wikipedia-Editor. Average accuracy is computed out of 10 runs.

this happens for extreme cases where either the number of eigenvectors is small, or when the amount of labeled nodes is limited, which is consistent with observations presented in [6].

5. Conclusion. Signed networks have become increasingly important in the modelling of social and other phenomena. The classification of nodes in signed networks has only recently become of interest and we illustrate that a technique previously introduced for classification of classical graph data can be extended to signed networks. For this we proposed the use of several different graph Laplacians and discussed their properties. We showed that these can be used with a diffuse interface approach on signed networks for smooth and non-smooth potentials. We then tested our technique on various real-world datasets and showed that the

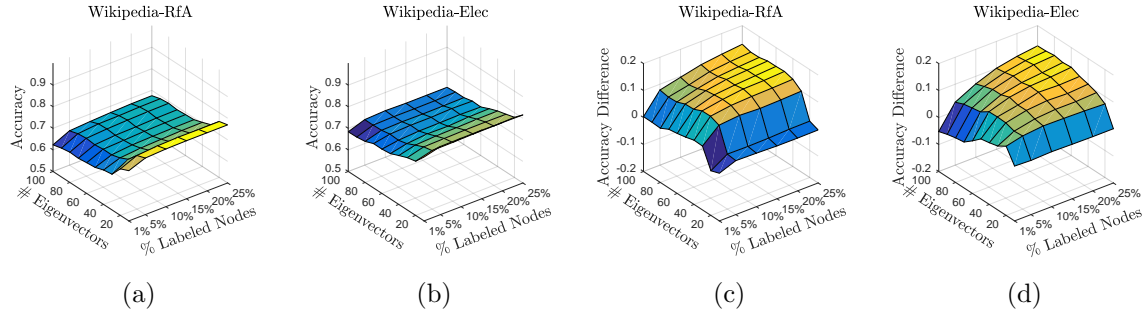


Figure 5: From left to right: Figures 5a and 5b show the average classification accuracy of our method based on the non-smooth potential and the signed normalized Laplacian L_{SN} under different number of eigenvectors and different amounts of labeled nodes. Figures 5c and 5d show the difference of accuracy between smooth and non-smooth potential models, where negative values mean that the non-smooth version outperforms the smooth version.

method performs well and compared with a competing approach performs favorably. For a small set of training data, the nonsmooth potential typically outperforms the smooth one.

REFERENCES

- [1] S. M. Allen and J. W. Cahn. A microscopic theory for antiphase boundary motion and its application to antiphase domain coarsening. *Acta Metall.*, 27(6):1085–1095, 1979.
- [2] A. L. Bertozzi, S. Esedoglu, and A. Gillette. Inpainting of binary images using the Cahn–Hilliard equation. *IEEE Trans. Image Process.*, 16(1):285–291, 2007.
- [3] A. L. Bertozzi and A. Flenner. Diffuse interface models on graphs for classification of high dimensional data. *Multiscale Model. Simul.*, 10(3):1090–1118, 2012.
- [4] J. F. Blowey and C. M. Elliott. Curvature dependent phase boundary motion and parabolic double obstacle problems. In *Degenerate diffusions (Minneapolis, MN, 1991)*, volume 47 of *IMA Vol. Math. Appl.*, pages 19–60. Springer, New York, 1993.
- [5] Jessica Bosch, David Kay, Martin Stoll, and Andy J. Wathen. Fast solvers for Cahn–Hilliard inpainting. *SIAM J. Imaging Sci.*, 7(1):67–97, 2014.
- [6] Jessica Bosch, Steffen Klamt, and Martin Stoll. Generalizing diffuse interface methods on graphs: non-smooth potentials and hypergraphs. *arXiv preprint arXiv:1611.06094*, 2016.
- [7] Jessica Bosch and Martin Stoll. A fractional inpainting model based on the vector-valued Cahn–Hilliard equation. *SIAM J. Imaging Sci.*, (4):2352–2382, 2015.
- [8] John W. Cahn and John E. Hilliard. Free energy of a nonuniform system. I. Interfacial free energy. *J. Chem. Phys.*, 28(2):258–267, 1958.
- [9] Y. Chen and X. Ye. Projection onto a simplex. *ArXiv e-prints:1101.6081*, 2011.
- [10] Kai-Yang Chiang, Joyce Jiyoung Whang, and Inderjit S Dhillon. Scalable clustering of signed networks using balance normalized cut. In *Proceedings of the 21st ACM international conference on Information and knowledge management*, pages 615–624. ACM, 2012.
- [11] Fan R. K. Chung. *Spectral graph theory*, volume 92 of *CBMS Regional Conference Series in Mathematics*. Amer. Math. Soc., Providence, RI, 1997.
- [12] Madhav Desai and Vasant Rao. A characterization of the smallest eigenvalue of a graph. *Journal of Graph Theory*, 18(2):181–194, 1994.
- [13] Julia A. Dobrosotskaya and Andrea L. Bertozzi. A wavelet-Laplace variational technique for image deconvolution and inpainting. *IEEE Trans. Image Process.*, 17(5):657–663, 2008.

-
- [14] P. Doreian and A. Mrvar. Partitioning signed social networks. *Social Networks*, 31(1):1–11, 2009.
 - [15] Patrick Doreian and Andrej Mrvar. Partitioning signed social networks. *Social Networks*, 31(1):1–11, 2009.
 - [16] Charles M. Elliott and Björn Stinner. Modeling and computation of two phase geometric biomembranes using surface finite elements. *J. Comput. Phys.*, 229(18):6585–6612, 2010.
 - [17] David J. Eyre. Unconditionally gradient stable time marching the Cahn–Hilliard equation. In *MRS Proceedings*, volume 529, page 39. Cambridge Univ Press, 1998.
 - [18] Jean Gallier. Spectral theory of unsigned and signed graphs. applications to graph clustering: a survey. *arXiv preprint arXiv:1601.04692*, 2016.
 - [19] C. Garcia-Cardona, E. Merkurjev, A. L. Bertozzi, A. Flenner, and A. G. Percus. Multiclass data segmentation using diffuse interface methods on graphs. *IEEE Trans. Pattern Anal. Mach. Intell.*, 36(8):1600–1613, 2014.
 - [20] Harald Garcke, Britta Nestler, Björn Stinner, and Frank Wendler. Allen-Cahn systems with volume constraints. *Math. Models Methods Appl. Sci.*, 18(8):1347–1381, 2008.
 - [21] Harald Garcke, Britta Nestler, and Barbara Stoth. A multi phase field concept: Numerical simulations of moving phase boundaries and multiple junctions. *SIAM J. Appl. Math.*, 60:295–315, 1999.
 - [22] Frank Harary et al. On the notion of balance of a signed graph. *The Michigan Mathematical Journal*, 2(2):143–146, 1953.
 - [23] M. Hintermüller, M. Hinze, and M. H. Tber. An adaptive finite-element Moreau–Yosida-based solver for a non-smooth Cahn–Hilliard problem. *Optim. Methods Softw.*, 26(4-5):777–811, 2011.
 - [24] M. Hintermüller, K. Ito, and K. Kunisch. The primal-dual active set strategy as a semismooth Newton method. *SIAM J. Optim.*, 13(3):865–888, 2002.
 - [25] Cho-Jui Hsieh, Kai-Yang Chiang, and Inderjit S Dhillon. Low rank modeling of signed networks. In *Proceedings of the 18th ACM SIGKDD international conference on Knowledge discovery and data mining*, pages 507–515. ACM, 2012.
 - [26] Andrew V Knyazev. Signed laplacian for spectral clustering revisited. *arXiv preprint arXiv:1701.01394*, 2017.
 - [27] S. Kropivnik and A. Mrvar. An Analysis of the Slovene Parliamentary Parties Networks. *Development in Statistics and Methodology*, pages 209–216, 1996.
 - [28] Srijan Kumar, Francesca Spezzano, and V.S. Subrahmanian. Vews: A wikipedia vandal early warning system. In *Proceedings of the 21th ACM SIGKDD international conference on Knowledge discovery and data mining*. ACM, 2015.
 - [29] Jérôme Kunegis, Andreas Lommatzsch, and Christian Bauckhage. The slashdot zoo: mining a social network with negative edges. In *Proceedings of the 18th international conference on World wide web*, pages 741–750. ACM, 2009.
 - [30] Jérôme Kunegis, Stephan Schmidt, Andreas Lommatzsch, Jürgen Lerner, Ernesto William De Luca, and Sahin Albayrak. Spectral analysis of signed graphs for clustering, prediction and visualization. In *SDM*, volume 10, pages 559–559. SIAM, 2010.
 - [31] Jure Leskovec, Daniel Huttenlocher, and Jon Kleinberg. Predicting positive and negative links in online social networks. In *Proceedings of the 19th international conference on World wide web*, pages 641–650. ACM, 2010.
 - [32] Jure Leskovec, Daniel Huttenlocher, and Jon Kleinberg. Signed networks in social media. In *Proceedings of the SIGCHI conference on human factors in computing systems*, pages 1361–1370. ACM, 2010.
 - [33] Jure Leskovec and Andrej Krevl. SNAP Datasets: Stanford Large Network Dataset Collection. <http://snap.stanford.edu/data>, June 2014.
 - [34] Yibao Li, Darae Jeong, Jung-il Choi, Seunggyu Lee, and Junseok Kim. Fast local image inpainting based on the Allen–Cahn model. *Digit. Signal Process.*, 37:65–74, 2015.
 - [35] XIYANG Luo and ANDREA L. Bertozzi. Convergence analysis of the graph Allen–Cahn scheme. Technical report, Dept. Math., Univ. of California Los Angeles, Los Angeles, CA, 2016.
 - [36] Pedro Mercado, Francesco Tudisco, and Matthias Hein. Clustering Signed Networks with the Geometric Mean of Laplacians. In *Advances in Neural Information Processing Systems*, pages 4421–4429, 2016.
 - [37] E. Merkurjev, C. Garcia-Cardona, A. L. Bertozzi, A. Flenner, and A. G. Percus. Diffuse interface methods for multiclass segmentation of high-dimensional data. *Appl. Math. Lett.*, 33:29–34, 2014.
 - [38] Ekaterina Merkurjev, Tijana Kostić, and Andrea L. Bertozzi. An MBO scheme on graphs for classification

- and image processing. *SIAM J. Imaging Sci.*, 6(4):1903–1930, 2013.
- [39] K. E. Read. Cultures of the Central Highlands, New Guinea. *Southwestern Journal of Anthropology*, 10(1):pp. 1–43, 1954.
 - [40] Carola-Bibiane Schönlieb and Andrea L. Bertozzi. Unconditionally stable schemes for higher order inpainting. *Commun. Math. Sci.*, 9(2):413–457, 2011.
 - [41] David I Shuman, Sunil K Narang, Pascal Frossard, Antonio Ortega, and Pierre Vandergheynst. The emerging field of signal processing on graphs: Extending high-dimensional data analysis to networks and other irregular domains. *IEEE Signal Processing Mag.*, 30(3):83–98, 2013.
 - [42] Jiliang Tang, Charu Aggarwal, and Huan Liu. Node classification in signed social networks. In *Proceedings of the 2016 SIAM International Conference on Data Mining*, pages 54–62. SIAM, 2016.
 - [43] J. E. Taylor and J. W. Cahn. Linking anisotropic sharp and diffuse surface motion laws via gradient flows. *J. Statist. Phys.*, 77(1-2):183–197, 1994.
 - [44] Yves van Gennip, Nestor Guillen, Braxton Osting, and Andrea L. Bertozzi. Mean curvature, threshold dynamics, and phase field theory on finite graphs. *Milan J. Math.*, 82(1):3–65, 2014.
 - [45] Ulrike von Luxburg. A tutorial on spectral clustering. *Stat. Comput.*, 17(4):395–416, 2007.
 - [46] Xiaoqiang Wang and Qiang Du. Modelling and simulations of multi-component lipid membranes and open membranes via diffuse interface approaches. *J. Math. Biol.*, 56(3):347–371, 2008.
 - [47] Shuhan Yuan, Xintao Wu, and Yang Xiang. *SNE: Signed Network Embedding*, pages 183–195. Springer International Publishing, Cham, 2017.
 - [48] Dengyong Zhou and Bernhard Schölkopf. A regularization framework for learning from graph data. In *ICML Workshop on Statistical Relational Learning*, pages 132–137, 2004.